Eur. Phys. J. Appl. Phys. **42**, 47–53 (2008)
DOI: 10.1051/epjap:2008021

THE EUROPEAN PHYSICAL JOURNAL APPLIED PHYSICS

Pinus Pinaster surface treatment realized in spatial and temporal afterglow DBD conditions

E. Lecoq[1], F. Clément[1], E. Panousis[1], J.-F. Loiseau[1], B. Held[1], A. Castetbon[2], and C. Guimon[3,a]

[1] Laboratoire d'Electronique des Gaz et des Plasmas, Université de Pau et des Pays de l'Adour, 64000 Pau, France
[2] Institut Pluridisciplinaire de Recherche sur l'Environnement et les Matériaux, IPREM, Equipe Chimie Analytique Bio Inorganique et Environnement (ECABIE), UMR (CNRS) 5254, Université de Pau et des Pays de l'Adour, 64000 Pau, France
[3] Institut Pluridisciplinaire de Recherche sur l'Environnement et les Matériaux, IPREM, Équipe Chimie Physique (ECP), UMR (CNRS) 5254, Université de Pau et des Pays de l'Adour, 64000 Pau, France

Received: 5 July 2007 / Received in final form: 15 October 2007 / Accepted: 15 January 2008
Published online: 19 March 2008 –

Abstract. This experimental work deals with the exposition of Pinus Pinaster wood samples to a DBD afterglow. Electrical parameters like duty cycle and injected energy in the gas are being varied and the modifications induced by the afterglow on the wood are analysed by several macroscopic and microscopic ways like wettability, XPS analyses and also soaking tests of treated wood in a commercial fungicide solution. Soaking tests show that plasma treatment could enhance the absorption of fungicide into the wood. The wettability results point out that the plasma treatment can inflict on the wood different surface properties, making it hydrophilic or hydrophobic, when varying electrical parameters. XPS analyses reveal several chemical modifications like an increase of the O/C ratio and the presence of carboxyl groups on the surface after plasma treatments.

PACS. 52.75.-d Plasma devices – 81.65.-b Surface treatments – 82.80.Pv Electron spectroscopy (X-ray photoelectron (XPS), Auger electron spectroscopy (AES), etc.)

1 Introduction

When exposed to natural outdoor conditions with variations of temperature and humidity, wood samples are subject to contamination by fungi and particularly by blue stain fungi which are responsible of bluish or greyish discoloration on the wood, causing economical losses in sawmills.

To avoid this type of degradation, traditional methods usually involve the use of chemical polluting biocides [1–3]. Last years, because of environmental constraints, the wood industry was forced to develop environmentally friendly products or non-biocidal alternatives.

Consequently, some less polluting products have been developed. However, these products have not attained the necessary degree of efficiency: impregnation by soaking is not optimal and most of the time, the treatment has a short-term effect because there are no chemical interactions between fungicides and wood [3].

Another alternative to prevent wood degradation by fungi is heat treatment which leads to modification of some chemical properties of wood and reduces its moisture taking-back. Nevertheless, with this type of treatment, the increase of durability is effective to the detriment of mechanical properties of wood [4–7].

Cold plasma technology is now used in many fields to modify surface properties of many types of materials, without affecting their bulk properties and with no polluting rejections [8–11]. By using a Dielectric Barrier Discharge (DBD) it is possible to generate a cold plasma at atmospheric pressure conditions [12–14]. Moreover, the technology called "plasma jet" in the literature offers, with the use of high gas flow, the possibility to transport reactive species outside the discharge gap and towards the surface [15–17]. Consequently, by coupling these two technologies (DBD and plasma jet), it is possible to generate great amounts of reactive gas at atmospheric pressure. Furthermore, a particularity of the set-up used here is that by using an HV chopping system, temporal afterglow conditions are achieved as well. Thus, it can be suggested that the treatment is realised in spatio-temporal afterglow conditions.

The use of this type of chemically active gas appears as a solution to reduce wood fungi contamination. Indeed, a plasma treatment could lead to wood surface modifications which may change the behaviour of wood surfaces regarding to fungicides or also have an influence on the development and fixation of fungi on the surface.

[a] e-mail: jean-francis.loiseau@univ-pau.fr

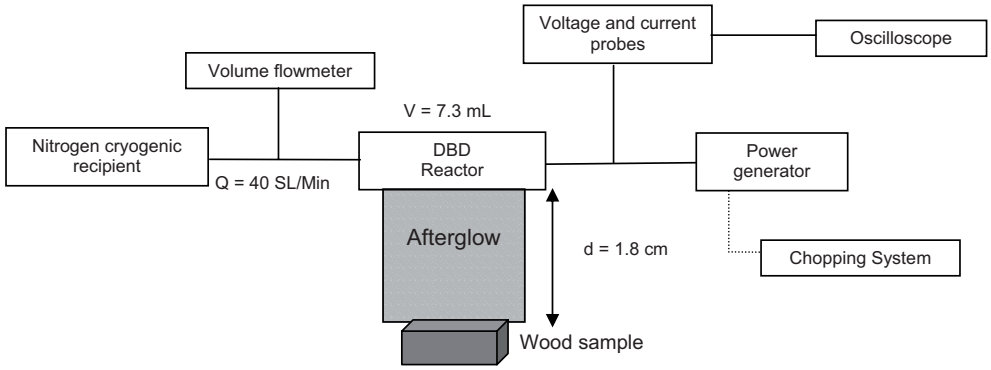

Fig. 1. Scheme of the experimental set-up.

The present study can be divided in two parts. The first approach consists in analysing what happens when a block of wood, treated in spatial and temporal DBD afterglow conditions, is soaked in a commercial fungicide used in the industry, in terms of absorption and fixation. Mass measurements and acid-base titration were used for this first approach.

In the second approach, the aim is to characterize Pinus Pinaster surfaces before and after plasma treatment. The experiments were carried out in order to determine the effect of a few electrical parameters on the treatment which was characterized by wettability and XPS analyses.

2 Material and methods

2.1 Wood samples

The wood used in the study is Pinus Pinaster with a humidity of 10–12%. Treatment was performed on blocks of $45 \times 25 \times 20$ mm for wettability measurements and soaking tests and $10 \times 10 \times 2$ mm for XPS analyses.

2.2 Experimental set up for plasma treatment

The scheme of the experimental set up is presented in Figure 1 and has already been described in a previous paper [8].

The gas used is nitrogen. It is provided by a cryogenic vessel (CRYOVAP 200) and the gas flow is controlled by a volume flowmeter (Analyt-MTC 0–100 SL/min), located just at the gas inlet of the DBD reactor. For the whole study, the gas flow was fixed at 40 SL/min.

The reactor has a cylindrical coaxial geometry. The H.V. signal is applied on the inner electrode which is coated with a dielectric, while the outer electrode is grounded. The volume of the reactor is of 7.3 ml and the gas is exiting through a narrow slit extending on one of the sides of the reactor, forming an afterglow with rectangular section shown in Figure 1.

The reactor is electrically supplied by a power generator which delivers quasi sinusoidal voltage and current waveforms in a frequency value of about 130 kHz. The total circuit current $i(t)$ and the applied voltage $v(t)$ are measured at the output of the generator and visualized with an oscilloscope (Tektronix 3034 B, 250 MHz, 2.5 Gs/s). Consequently, the mean electrical power $P = \langle p(t) \rangle$, injected into the system can be controlled during all the treatments. For this study, the injected power has been kept constant at a value of 900 W.

A chopping system has been added to the power generator in order to form successive voltage ON and voltage OFF phases of adjustable duration. As a result, we worked on the duty cycle and on the treatment time to vary the injected energy.

The treatment chamber is a custom-made vessel where the samples can be placed at various distances from the plasma jet output. The two parts developed in this study (soaking tests and surface characterization) involve two devices to treat the samples. For soaking tests, 4 faces on 6 of each sample are treated (2 faces of $25 \times 45 = 1125$ mm^2 in area and 2 faces of $20 \times 45 = 900$ mm^2 in area). The untreated faces correspond to the extremities of the sample (area of $20 \times 25 = 500$ mm^2). For that, the sample is positioned under the slit of the reactor, held by one of the extremities, and is rotating thanks to a small AC motor at a 3.33 rpm. On the other hand, for surface characterization, only one face (area of $25 \times 45 = 1125$ mm^2) is treated, the sample staying fixed below the reactor's slit.

The distance between the exit of the reactor and the sample was the same for all treatments ($d = 1.8$ cm). The pressure in the vessel is 1 Bar and the gas is evacuated by an air extraction device.

2.3 Soaking tests

The fungicide used is a commercial product used in wood industry. According to the manufacturer, it contains 14% w/w trimethylcocoammonium chloride and 5.2% w/w borax as active agents to prevent wood contamination and also 26% w/w ethyl-2-hexanoate sodium salts, allowing a better interface between the wood and the solution. Analyses realized by acid-base titration showed that there is also a part of sodium hydroxide in the solution. Prior to use, the product is diluted at 6% w/w in distilled water.

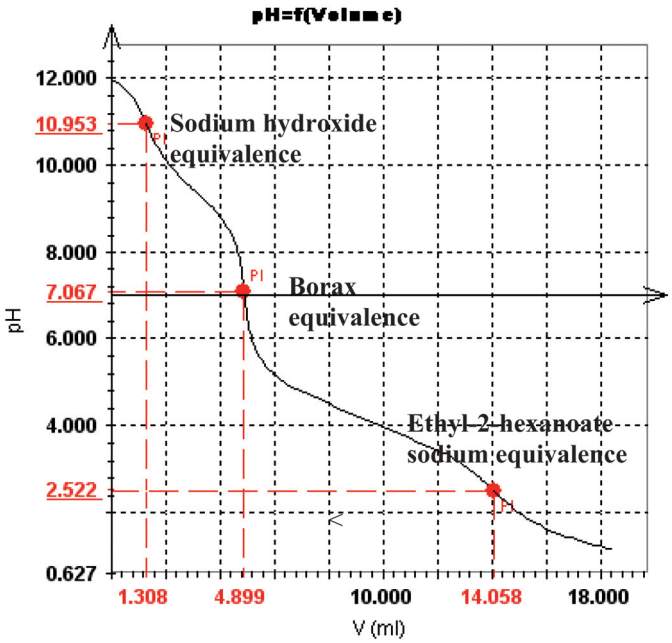

Fig. 2. Characteristic curve obtained by acid-base titration of fungicide solutions.

2.3.1 Mass measurements

Measurements of the wood samples' mass are made before and after treatments so that a mass loss in percent (M_L) is calculated.

After mass measurements, samples are soaked in the fungicide solution for 1 min, and the mass after soaking is measured to determine the mass of fungicide (M^{abs}) absorbed by samples. From these measurements an absorption parameter C_{abs} was established following:

$$C_{abs} = \frac{M_{tr}^{abs} - M_0^{abs}}{M_0^{abs}} \times 100 \qquad (1)$$

where M_{tr}^{abs} and M_0^{abs} are respectively the fungicide mass absorbed by treated and untreated samples.

2.3.2 Acid-base titration

The fungicide solutions were titrated using a pH titration workstation (TitraLab TIM960 — Radiometer Analytical — France) with HCl 0.1 N as reagent. A typical curve obtained is presented in Figure 2. pH measurement as a function of the HCl volume added in the solution results in the determination of equivalent volumes (points noted PI for inflection point) used for calculation of sodium hydroxide, borax and ethyl-2-hexanoate sodium concentrations. Measurements were realized in DET mode (Dynamic Equivalent point Titration).

Solutions were titrated before and after soaking of treated and untreated wood blocks. This part of the study consists in the determination on whether the solution is absorbed in an homogeneous way by wood samples or if some of the species are preferentially absorbed, changing their content in the solution after soaking.

2.4 Surface characterization methods

2.4.1 Water contact angle measurements

Water contact angles were determined by the sessile drop method, using a Digidrop (GBX-France). 8 drops (5 μl) of de-ionized water were deposited on each sample: four on the middle of the sample (which is situated just below the slit of the reactor) and four on the sides. Experiments were repeated twice for each type of treatment. Before the deposing of the drop, samples were left 2 min under gas flow (40 SL/min) and 8 min at ambient air to cool down. This time is sufficient to obtain a surface temperature approximately equal to the room temperature for all treatments.

When the water drop is deposited on untreated wood surface, two different steps can be distinguished. During the first one, the liquid spreads on the surface (wetting) but it also penetrates in the wood cell lumens. During the second one, the liquid does not spread anymore on the surface, but it still penetrates, until the drop is totally absorbed [18]. The study of the contact angle value and the drop baseline width with time just after the deposit of the drop showed that the end of the first step is reached after 10 s. Consequently, we chose this time to measure the value of the contact angle.

2.4.2 XPS analyses

The XPS spectra were recorded using an SSI M-Probe spectrometer at room temperature. Monochromatic Al K_α X-rays (1486.6 eV) were used for the excitation and the analysis chamber pressure was approximately 10^{-9} mbar. Being given the humidity of wood, approximately 20 h were needed to reach the necessary vacuum for the analysis. Survey spectra were recorded at constant pass energies of 150 eV and 50 eV for high-resolution analysis. Experimental and theoretical bands were fitted (80% Gaussian and 20% Lorentzian) using a non-linear baseline [19] with a least-squares algorithm. Quantitative analyses were calculated using Scofield factors [20] and binding energies were determined using the C_{1s} binding energy of aliphatic carbon (284.6 eV) as the reference, with an experimental error of ± 0.2 eV. Charge effects were compensated by the use of a flood gun (5 eV).

3 Results

3.1 Soaking tests

Figure 3 shows the mass loss in percent (M_L) as a function of injected energy for $r_c = 1$, denoting that the variation of injected energy is obtained by variation of treatment time. Results show that M_L increases with injected energy. This mass loss may be attributed to water evaporation induced by thermal energy dissipated during the treatment. Alternatively, it can also be the result of partial degradation of the wood, due to thermal energy or chemical reactions.

Table 1. Sodium hydroxide, Borax and Ethyl-2-hexanoate concentrations in fungicide solutions before and after soaking, for treated and untreated samples, determined by acid-base titration.

	Concentrations (mol.L^{-1})		
Titrated solutions	Sodium hydroxide	Borax	Ethyl-2-hexanoate sodium
Before soaking	0.0138 ± 5.10^{-4}	0.0177 ± 3.10^{-4}	0.0901 ± 1.10^{-3}
After soaking of an untreated sample	0.0136 ± 2.10^{-4}	0.0176 ± 5.10^{-4}	0.0894 ± 2.10^{-3}
After soaking of a treated sample ($E = 32.4$ kJ)	0.0135 ± 4.10^{-4}	0.0182 ± 6.10^{-4}	0.0904 ± 1.10^{-3}
After soaking of a treated sample ($E = 162$ kJ)	0.0141 ± 5.10^{-4}	0.0171 ± 5.10^{-4}	0.0899 ± 3.10^{-3}

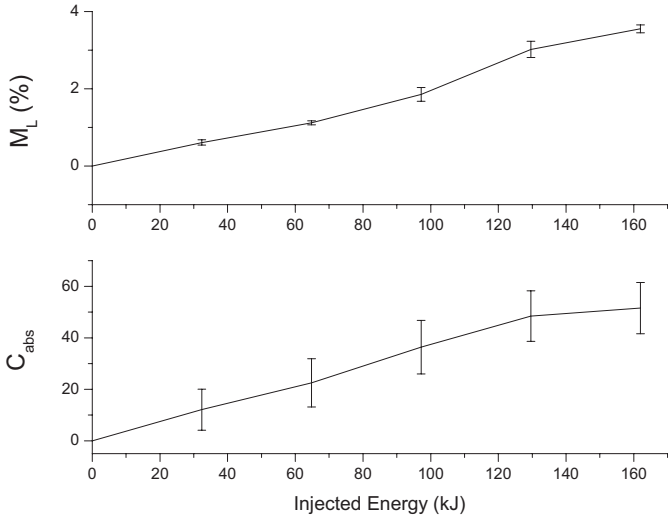

Fig. 3. Mass loss during treatment (M_L) and absorption parameter (C_{abs}) as a function of injected energy ($d = 1.8$ cm, $P = 900$ W, $r_c = 1$, $Q = 40$ SL/min).

$$\left(C_{abs} = \frac{M_{tr}^{abs} - M_0^{abs}}{M_0^{abs}} \times 100 \quad \text{et} \quad M_L = \frac{(M_i - M_f)}{M_i} \times 100\right)$$

where M_i and M_f are respectively the initial (before treatment) and the final (after treatment) mass of the samples and M_{tr}^{abs} and M_0^{abs} the fungicide mass absorbed by treated and untreated samples.

According to literature, degradation of hemicelluloses can lead to the formation of formic acid, acetic acid and furfural, which are volatile compounds [4].

Figure 3 also points out that higher the injected energy during treatment, the higher the absorption parameter is. It has to be noticed that if the injected energy is increased, the temperature of the sample at the end of the treatments is higher. As a consequence, improvement of fungicide absorption in the wood could be the result of an increase in samples temperature. A better absorption of fungicide may also be due to modifications of the surface which may enhance the interactions between wood and fungicide.

Results of acid-base titration of fungicide solutions before and after soaking, for treated and untreated samples

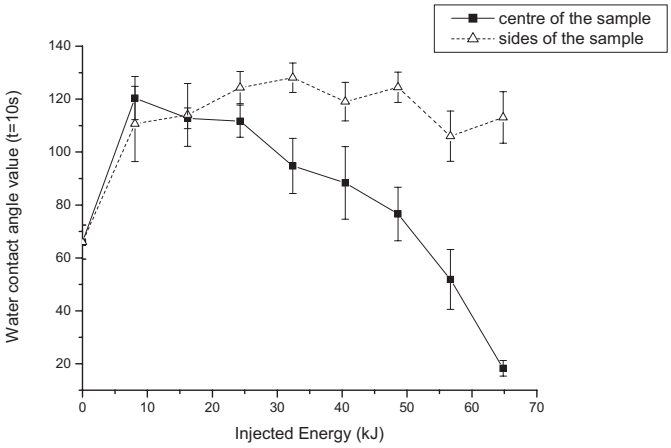

Fig. 4. Water contact angle value 10 s after the deposit of the drop as a function of injected energy on the centre and on the sides of the sample ($d = 1.8$ cm, $P = 900$ W, $r_c = 1$, $Q = 40$ SL/min).

are presented in Table 1. It shows that sodium hydroxide, borax and ethyl-2-hexanoate sodium contents where the same in all solutions. It means that the fungicide product is absorbed in a homogeneous way, with no preferential migration of some compounds in the wood.

3.2 Water contact angles measurements

3.2.1 Influence of the injected energy

Figure 4 displays the evolution of the water contact angle measured 10 s after the deposit of the drop as a function of the injected energy without chopping system ($r_c = 1$). The average contact angle obtained on untreated surfaces is about 65°. We can observe that the plasma treatment leads to noteworthy modifications in terms of water wettability.

When the injected energy is low (until approximately 30 kJ), the treatment results in a hydrophobic character of the surface. In these cases, the contact angle values are about 110−120°: the drop does not spread nor even is absorbed.

Table 2. Surface composition of the samples for the different treatments ($d = 1.8$ cm, $P = 900$ W, $r_c = 1$, $Q = 40$ SL/min).

	Atomic percentage						Atomic ratio	
Injected energy (kJ)	O	C	N	Ca	Na	K	O/C	N/C
0	29.5	69.7	0.6	0.1	0.2	0.0	0.42383	0.0079
16.2	39.9	57.3	1.4	0.3	1.2	0.2	0.69581	0.02373
27	40.1	56.6	1.6	0.4	1.0	0.2	0.70735	0.02861
54	40.0	54.7	1.2	1.4	2.5	0.3	0.73102	0.02251
64.8	36.6	63.3	1.0	0.4	0.6	0.2	0.57819	0.01579
108	41.0	52.5	1.1	0.4	5.7	0.6	0.78072	0.0207

Table 3. Components of C_{1s} peak for the different treatments ($d = 1.8$ cm, $P = 900$ W, $r_c = 1$, $Q = 40$ SL/min).

	Proportions (%) of carbon contributions			
Injected energy (kJ)	C_1: C–C/C–H	C_2: C–O/C–N	C_3: C=O	C_4: O–C=O
0	53	40	8	0
16.2	22	50	17	11
27	22	52	17	9
54	34	42	17	8
64.8	36	44	14	6
108	36	39	17	9

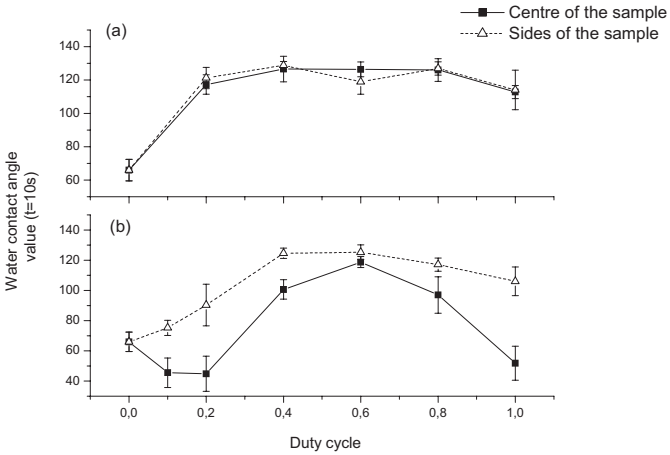

Fig. 5. Water contact angle value 10 s after the deposit of the drop as a function of the duty cycle on the centre and on the sides of the sample ($d = 1.8$ cm, $P = 900$ W, $Q = 40$ SL/min, $E = 16.2$ kJ (a) and $E = 56.7$ kJ (b)).

The increase in injected energy leads to distinct behaviours between the centre and the sides of the sample. The contact angle value decreases with the increase of the injected energy on the centre, while on the sides, the treatment makes the surface hydrophobic whatever the injected energy is.

3.2.2 Influence of the duty cycle r_c

Figure 5 shows the evolution of the water contact angle as a function of the duty cycle for injected energy values of 16.2 kJ and 56.7 kJ for which we had observed two behaviours of the water drop totally different at the centre of the sample.

It can be observed that when the injected energy is quite low (16.2 kJ), the duty cycle has no influence on the water contact angle value. The surface presents a hydrophobic behaviour, whatever the duty cycle is, on the centre like on the sides.

On the contrary, the duty cycle seems to have an influence on the value of the water contact angle when the injected energy is higher. At the centre of the sample, for intermediate duty cycles ($r_c = 0.4$, 0.6 and 0.8) the water contact angle values are higher and the surface has a hydrophobic behaviour. Nevertheless, for low duty cycles ($r_c = 0.1$ and 0.2) and for $r_c = 1$, the water contact angle decreases and the surface presents a hydrophilic character.

3.3 XPS study

XPS analyses have been realized in order to have a possible understanding of the afterglow microscopic effect on the surface. Surface composition results are summarized in Table 2. In this analysis, we focused on the resolution of the C_{1s} peak. According to literature [5,21,22], four peaks may appear, generally expressed as $C_1 - C_4$. These carbon bands are interpreted to be C–C/C–H (C_1), C–O/C–N (C_2), C=O (C_3) and O=C–O (C_4). Proportions of these contributions for the samples studied are detailed in Table 3.

We can see in Table 2 that the ratio of the atomic concentration of oxygen to carbon strongly increases after treatments. In the same way, the atomic percentage of nitrogen to carbon increases too.

Table 2 reveals also an increase of the proportion of cations like sodium, calcium and potassium on the surface with injected energy. These elements are naturally present in the wood bulk (∼1%) and they might migrate to the surface during/after the treatment [23].

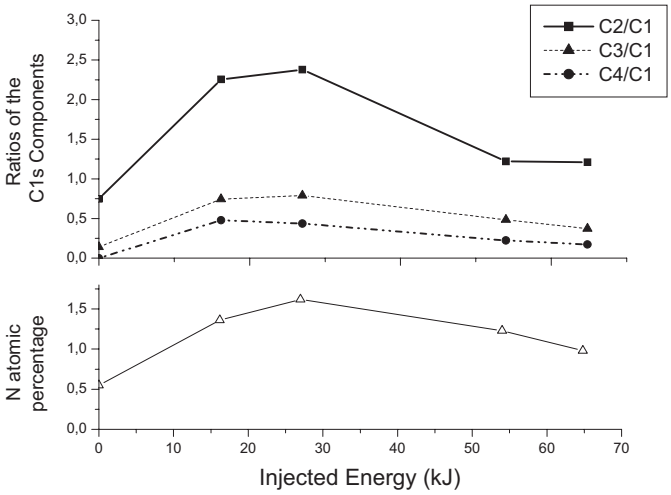

Fig. 6. Evolution of the C_2/C_1, C_3/C_1 and C_4/C_1 ratios and Nitrogen atomic percentage as a function of the injected energy ($d = 1.8$ cm, $P = 900$ W, $r_c = 1$, $Q = 40$ SL/min).

Table 3 shows that there are some differences in proportions of carbon contributions after treatment. We can note a strong decrease of the C_1 component after treatment, particularly for lower injected energies, and also the apparition of the C_4 component, implying the presence of carboxyl groups on the surface.

Figure 6 presents the evolution of the C_2/C_1, C_3/C_1 and C_4/C_1 ratios as a function of the injected energy. For lower injected energies, these ratios are larger than before treatment and they tend to decrease when the injected energy is amplified. We can observe the same evolution of the nitrogen atomic percentage.

4 Discussion

We saw that the treatment in spatial and temporal afterglow DBD conditions could lead to surface modifications on Pinus Pinaster. Water wettability tests show that we can inflict on the wood surface distinct surface properties, making it hydrophilic or hydrophobic when varying electrical parameters and XPS analyses reveal chemical surface modifications after plasma treatments.

In the light of the results here presented and according to the literature, a number of mechanisms, hereafter detailed, can be thought to be occurring during wood surface treatment by the DBD afterglow. It should be beforehand underlined, however, that the following remains strictly hypothetical since further experimental studies are needed for confirmation or exclusion.

Heat treatments usually make wood surface hydrophobic. Numerous authors give several explanations to this phenomenon [4–7,18,24]. The most frequently evoked explanation is the migration of wood extractives from the bulk to the surface. These extractives are often resins or also low molecular weight fatty acids (acetic acid and formic acid) issued from degradation of hemicelluloses which are water repellent. The results obtained by XPS in this study show that the treatment induces formation of O−C=O bonds at the surface, which could reveal the presence of carboxylic acids and consequently may explain the hydrophobic behaviour observed by sessile drop tests for certain electrical parameters and particularly for low injected energies. When increasing injected energy, the wood surface totally changes and becomes hydrophilic. For those higher energies, we see by XPS that the C_4/C_1 ratio decreases and it may be explained by a vaporisation or degradation of formic acid and acetic acid because of the increase of temperature and a longer treatment time. That would also explain the increase of M_L observed with increasing energy at Section 3.1.

The literature shows also that hemicelluloses are in great part responsible of wood hygroscopic and hydrophilic behaviour because of their free hydroxyl groups. Some authors reported that when wood is heated, ether links are formed by splitting of two adjacent hydroxyl groups, leading to a reduction of wood hygroscopy and hydrophily [4–6]. This phenomenon may happen during the DBD afterglow treatment but it can not be distinguished by XPS analyses because both carbons bonded to hydroxyl groups or present in ether groups correspond to the C_2 band. However, when comparing contact angles measured on treated surfaces and C_2/C_1 ratio, a correlation can be observed. In fact, contact angles values fall with decreasing of C_2/C_1 ratio. An increase of injected energy may lead to the breaking of ether linkages, making the wood becoming more hydrophilic.

Another theory proposed to explain water repellence after heat treatment or drying evokes molecular reorientations which can occur at the surface [24]. Indeed, it is known that synthetic polymers molecules on the surface can reorient to present lower or higher surface energy, particularly when plasma-treated [25–27]. In the case of wood, we know that it presents both very hydrophilic parts and hydrophobic parts. As a consequence, molecular reorientation should be a significant factor to explain an increase or a decrease in wettability. Duty cycle, injected energy and treatment time could influence the mechanisms in molecules reorientation and that should lead to different steps of treatment and explain the differences observed in Section 3.2.

Some authors also evoke a closure of large micropores in cell walls [24]. Indeed, changes in cristallinity of cellulose or conformational reorganization of polymeric components of wood could lead to more perfectly aligned bonds which may no longer be separable by intrusion of water. That would explain why water drops are not absorbed in the wood for certain electrical parameters as seen during wettability tests. This hypothesis is in agreement with results obtained by Blantocas et al. [28,29]. They exposed wood samples to low energy hydrogen ion showers issued from a Gas Discharge Ion Source (GDIS) and observed by scanning electron micrographs partial closure of surface pores. Moreover, they found that ion beam irradiation made the surface hydrophobic for low energies and hydrophilic for higher energies.

5 Conclusion

The first part of the study, consisting in soaking tests in the commercial fungicide product, showed that the absorption parameter is improved with treatment. At this step, we are not in measure to explain why, but we can suppose that chemical surface modifications allow a better interface between wood and product, making it penetrate more easily into the wood structure. However, further studies are needed in order to determine if the product presents a better fixation on afterglow-modified surfaces.

Concerning the surface characterization, several hypotheses were made to explain the fact that wood surface becomes either hydrophobic or either hydrophilic depending on experimental electrical parameters.

A parallel work, dealing with the optical study of the same DBD afterglow, in order to identify species present in the afterglow [30] is currently carried on. It will be now essential to try to understand how these reactive species can interact with the wood surface to lead to the modifications exposed before.

This work is financially supplied by the French national research program ANR – Plasmapal and by a French national partnership (CIFRE convention: ANRT- Beynel-Manustock Society (Belin-Beliet, France) – LEGP). The staff of the Atelier de Physique of Pau University is gratefully acknowledged for his technical help.

References

1. J.A. Hingston, C.D. Collins, R.J. Murhy, J.N. Lester, Env. Pollut. **111**, 53 (2001)
2. T. Townsend, B. Dubey, T. Tolaymat, H. Solo-Gabriele, J. Env. Manag. **75**, 105 (2005)
3. E. Baysal, A. Sonmez, M. Colak, H. Toker, Biores. Tech. **97**, 2271 (2006)
4. S. Mouras, P. Girard, P. Rousset, P. Permadi, D. Dirol, G. Labat, Ann. For. Sci. **59**, 317 (2002)
5. P. Gérardin, M. Petric, M. Petrissans, J. Lambert, J.J. Ehrhrardt, Polym. Degr. Stabil. **92**, 653 (2007)
6. D.P. Kamdem, A. Pizzi, A. Jermannaud, Holz als Roh- und Werkstoff **60**, 1 (2002)
7. M. Hakkou, M. Pétrissans, A. Zoulalian, P. Gérardin, Polym. Degr. Stabl. **89**, 1 (2005)
8. E. Panousis, F. Clement, J.F. Loiseau, N. Spyrou, B. Held, J. Larrieu, E. Lecoq, C. Guimon, Surf. Coat. Tech. **201**, 7292 (2007)
9. X. Liu, P.K. Chu, C. Ding, Mat. Sci. Eng. **47**, 49 (2004)
10. G. Borcia, C.A. Anderson, N.M.D. Brown, Plasma Sour. Sci. Technol. **12**, 335 (2003)
11. P. Rehn, A. Wolkenhauer, M. Bente, S. Förster, W. Viöl, Surf. Coat. Tech. **174-175**, 515 (2003)
12. F. Massines, P. Segur, N. Gherardi, C. Khamphan, A. Ricard, Surf. Coat. Tech. **174-175**, 8 (2003)
13. J.M. Thiébault, T. Belmonte, D. Chaleix, P. Choquet, G. Baravian, V. Puech, H. Michel, Surf. Coat. Tech. **169-170**, 186 (2003)
14. H.E. Wagner, R. Brandenurg, K.V. Kozlov, A. Sonnenfeld, P. Michel, J.F. Behnke, Vacuum **71**, 417 (2003)
15. A. Schütze, J.Y. Jeong, S.E. Babayan, J. Park, G.S. Selwyn, R.F. Hicks, IEEE Trans. Plasma Sci. **26**, 1685 (1998)
16. C. Cheng, Z. Liye, R.J. Zhan, Surf. Coat. Tech. **200**, 6659 (2006)
17. S. Förster, C. Mohr, W. Viöl, Surf. Coat. Tech. **200**, 827 (2005)
18. Scheikl, M. Dunky, Holzforschung **52**, 89 (1998)
19. D.A. Shirley, Phys. Rev. B **5**, 4709 (1972)
20. J.H. Scofield, J. Electron Spectrosc. Relat. Phenom. **8**, 129 (1976)
21. Q. Shen, P. Mikkola, J.B. Rosenholm, Colloids and Surfaces A: Physicochem. Engineer. Aspects **145**, 235 (1998)
22. M. Jaic, R. Zivanovic, T. Stevanovic-Janezic, A. Dekanski, Holz als Roh- und Werstoff **54**, 37 (1996)
23. D. Dirol, X. Deglise, *Durabilité des bois* (Hermès Sciences Publications, 2001), p. 415
24. A.W. Christiansen, Wood and Fiber Science **22**, 441 (1990)
25. R. Morent, N. De Geyter, C. Leys, L. Gengembre, E. Payen, Surf. Coat. Technol. (2007). doi: 10.1016/j.surfcoat.2007.03.018
26. H. Yasuda, A.K. Sharma, T. Yasuda, J. Polym. Sci. Phys. Ed. **19**, 1285 (2003)
27. F. Clément, B. Held, N. Soulem, H. Martinez, Eur. Phys. J. Appl. Phys. **21**, 59 (2003)
28. G.Q. Blantocas, H.J. Ramos, M. Wada, Japanese J. Appl. Phys. **45**, 8498 (2006)
29. H.J. Ramos, J.L.C Monasterial, G.Q. Blantocas, Nucl. Instrum. Meth. Phys. Res. B **242**, 41 (2006)
30. A. Ricard, E. Panousis, F. Clement, T. Sinzdingre, J.-F. Loiseau, *Production of active species in a N_2 DBD Plasma afterglow at atmospheric gas pressure*, Eur. Phys. J. Appl. Phys., accepted (2008)